https://erjm.journals.ekb.eg
ISSN: 1110-1180

DOI: ---------

ERJ
Engineering Research Journal
Faculty of Engineering
Menoufia University

Effect of Changing Maximum Camber Position of the Turbine Blade on its Aerodynamic Performance

Eman M. Magdy[1]. Taher A. Sabry[2], Abdel-Hamid A. Abdel-Hamid[2], Ashraf A. Hussien[2*]

[1] Technical Support Engineer, Sanitary Drainage Company, Cairo, Egypt
[2] Mechanical Power Engineering Department, Faculty of Engineering, Menoufia University, Shebin El-kom, Egypt
[*](Corresponding author: as_amien@sh-eng.edu.eg)

ABSTRACT
This study presents numerical investigation for studying the effect of changing maximum camber position of turbine blade and different operating conditions on its aerodynamic performance and the flow pattern through turbine blade passage. Three different turbulence models, namely Standard k-ε, RNG k-ε, and Realizable k-ε are used to select the suitable turbulence model. Four turbine blades with different values of maximum camber position (t_m/C), namely 0.157, 0.23, 0.26 and 0.37 measured from blade leading edge are studied. The tested blade geometries are created and meshed by using ICEM, ANSYS software. The governing equations including mass, momentum, and energy equations are numerically solved using ANSYS Fluent 2017. Comparison of numerical results using the three different turbulence models with several published experimental data showed that the realizable k- ε turbulence model is suitable for simulating the flow characteristics through the turbine blade passage. The numerical results indicated that, changing the maximum camber position of the turbine blade significantly affects the pressure coefficient on the suction surface of the blade while its effect is small on the pressure surface of the turbine blade at different operating conditions. Finally, it can be concluded that, the best aerodynamic performance of the tested turbine blades, at constant values of, pitch-to-chord ratio of 0.9 and incidence angle of 0°, is achieved if the position of maximum camber of the turbine blades is located at approximately (x/C), 0.157 from the leading edge.

Keywords: *turbine blade, cascade, camber position, turbulence model, aerodynamic performance*.

1. Introduction

Turbomachinery blades are an integral part of air breathing propulsion systems, gas turbines, steam turbines and other energy conversion devices. The blade design is the most important process which affects the gas flow behavior and the blade performance, Turbine blade profiles with using Bezier curves technique have been presented in references [1,2]. The shape of blade profiles is controlled using the relative position of the control point with respect to the end points on the profile (leading and trailing edge), this technique allows creating the effective description of the known geometry of blade profile. Dunham [3] presented a parametric method of turbine blade profile design for an axial turbine, the shape of turbine blade is defined by an algebraic function of eight parameters: blade inlet and outlet angles, maximum thickness, trailing edge thickness, leading edge radius, and the points of maximum thickness and maximum camber. This method is believed to require less skill and experience than other methods that starting more directly take many mechanical or aerodynamic considerations. Pacciani [4] used the concept of laminar kinetic energy as a theoretical model for predicting high lift, at low Reynolds number of flow through turbine blade, the proposed model showed the ability to predict and evaluate the separated flow region including the bubble bursting and the flow separation. Large eddy simulation (LES) of flow and direct numerical method in low pressure turbine cascade were used to evaluate the blade performance [5,6]. The results indicated that large eddy simulation provides satisfactory performance. Jouini et al [7] studied experimentally aerodynamic performance of transonic turbine cascade at off design conditions. The experimental results showed a good agreement for testing blades near the design incidence. Sanz et al [8] presented numerical and experimental investigation of the wake flow downstream of a linear turbine cascade. Large discrepancies between

experimental and numerical data were observed due to periodic vortex shedding from the blunt trailing, which is not considered by turbulence model. The effects of stagger angle, and pitch chord on secondary flows downstream of turbine cascade have been studied in [9, 10]. The results indicated that pitch chord ratio and incidence angle have strongly influences on the profile efficiency, on the other hand stagger angle has a small effect. Zhou et al [11] studied experimentally aerodynamic performance for suction side and pressure side winglet cavity tips in a turbine blade cascade. The results showed that the winglet cavity has a better aerodynamic performance. Bode et al [12] investigated the effect of turbulence length scale on turbulence and transition in turbomachinery flows. The study proved a satisfactory turbulence dissipation rate and very good agreement with the measurement. Smooth curvature of airfoils for a general turbomachinery geometry has been presented in [13, 14]. The results showed that, the smooth connection between the leading and airfoil blade removes Mach number distribution peeks at the connection point. Nho et al. [15] determined the effects of turbine blade tip shape on total pressure losses and secondary flow of a linear turbine cascade. The results indicated that the total pressure coefficient increases as the tip clearance increases and at the same time the grooved pressure side tip has a good performance in total pressure loss reduction. The aerodynamic performance of the turbine cascade at different flow condition has been investigated by Sun et al [16]. The study concluded that the different flow condition has a limited influence on the velocity field as well as the outlet flow angle. Akolekar et al [17] presented the transition modelling for low pressure turbines using computational fluid dynamics driven machine learning, with using low pressure turbine T106A cascade. The results showed the ability of this model to accurately predict the flow coming off the blade trailing edge. Analysis of the influence of camber on hydrodynamic characteristic using Reynolds Averaged Navier Stokes method which coupled with the k-ε model RNG turbulence model has been studied by of Yining [18]. The results showed that airfoil's performance is affected by the overall geometry such as camber, thickness position of maximum relative thickness and position of maximum camber. Effect of camber and angles of attack on airfoil characteristics has been presented in [19]. The results showed that how the change of incidence angle and the position of camber affected blade performance, including efficiency, stall behavior and boundary layer development. Kim et al [20] investigated the effect of incidence angle variations on gas turbine blade performance. The results examined how the change in incidence angle influenced flow behavior, lift, drag, and stall characteristics. The results leaded to a better understanding of how incidence angle affects the aerodynamic performance of gas turbine blades. From the previous discussion it can be noted that the effect of changing maximum camber position of turbine blade on its aerodynamic performance needs more study to determine the best performance of turbine blades. Therefore, the main objective of present study is to numerically investigate to determine the aerodynamic performance and the flow pattern through turbine blade passage at different values of blade maximum camber positions with different operation conditions. Three different turbulence models, namely Standard k-ε, RNG k-ε, Realizable k-ε are used in this study. A comparison between numerical results of turbulence models and published experimental data will be performed to validate and select a suitable turbulence model. The numerical study is extended to determine the optimum value of the blade maximum camber position based on minimum value of pressure loss coefficient and maximum value of loading coefficient.

1- 2. Blade Generation

The blade geometry plays an important role on the performance of turbine blades. The geometry of blades is defined by a set of geometric and aerodynamic parameters, such as inlet and exit blade angles, axial chord, chord length, blade thickness and curvature of camber line. These parameters are used to specify and create 2-D blade profile. The effect of changing maximum camber position of the blade is studied for different four geometries. All geometries are created with the same procedures and steps to keep the same shape of blade pressure surface and cross section area as shown in Fig (1).

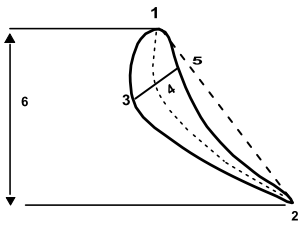

1-Leading edge
2-Trailing edge
3-Max. Camber position
4- Camber line
5-Chord line
6- Axial chord

Fig. (1) The shape of created blade

To change the maximum camber position of a turbine blade, three points are located on the suction surface of the reference turbine blade as shown in Fig. (1). The point (1) refers to leading edge and point (2) refers to trailing edge of the blade and they are fixed in the same locations. Point (3) is selected to determine the maximum camber (max. thickness) of the blade. The location of point (3) is movable to different locations on the suction surface of the blade with keeping a constant cross-sectional area. Four different blades are

created with different position of point (3) to describe the different values of camber position. Table 1 shows the name and position of the four tested blades.

Table (1) Definition of tested blades

Blade title	Symbol	Position of max. camber t_m/C
Geometry-1	G1	0.157
Geometry-2	G2	0.23
Geometry-3	G3	0.26
Geometry-4	G4	0.37

The different geometries of turbine blades are shown in Fig. (2). From the figure it can be observed that, all tested blades have the same leading and trailing edges points, chord length and shape of the pressure side.

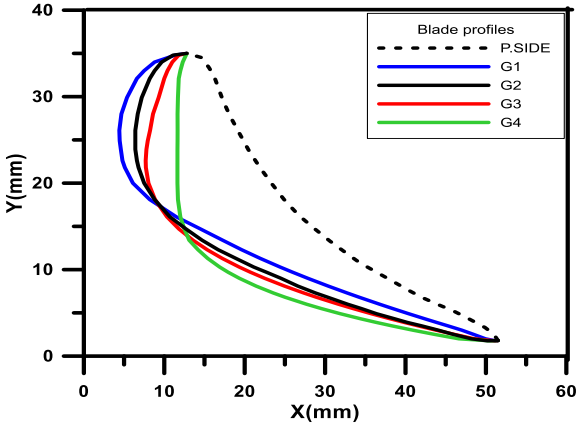

Fig. (2) Different geometries of tested blades.

3. Theoretical Analysis

Computational Fluid Dynamics is used to predict the fluid behaviour and aerodynamic performance of turbine blade using the Navier-Stokes equations. The domain is discretized using finite volumes method. ANSYS software is used to simulate the flow through the passage of turbine blades.

3-1 Governing equations

Conservation of mass and momentum equations of compressible flow accompanied with the equations of the selected turbulence models have been numerically solved using the commercial software ANSYS 17.0. The equations of mass, momentum and energy conservations used by the program can be written for the two dimensional (2-D) and steady flow as follows [21].

$$\frac{\partial}{\partial x}(\rho u\varphi)+\frac{\partial}{\partial y}(\rho v\varphi)=\frac{\partial}{\partial x}\left(\Gamma_\varphi\frac{\partial\varphi}{\partial x}\right)+\frac{\partial}{\partial y}\left(\Gamma_\varphi\frac{\partial\varphi}{\partial y}\right)+S_\varphi \quad \text{.....} \quad \textbf{(1)}$$

Here, φ is the dependent variable; while S_φ is the source term which has different expressions for different transport equations. The convection and diffusion terms for all the transport equations are identical. Γ_φ represents the diffusion coefficient for scalar variables and the effective viscosity μ_e for vectorial variables, (i.e. velocities). The characteristics of the transport equations are extremely useful when the equations are discretized (reduced to algebraic equations) and solved numerically. In fact, this equation also represents the continuity equation when $\varphi = 1$ and $S_\varphi = 0$.

Table (2) gives the expressions for the source terms S_φ for each dependent variable that are needed in solving conservation problems.

Table (2) Source terms in the transport equations

Equation	φ	Γ_φ	S_φ
Continuity	**1**	**0**	**0**
x-momentum	u	μ_e	$-\frac{\partial p}{\partial x}+\frac{\partial}{\partial x}\left(\mu_e\left(\frac{\partial u}{\partial x}-\frac{2}{3}\left(\frac{\partial u}{\partial x}+\frac{\partial v}{\partial y}\right)\right)\right)+\frac{\partial}{\partial y}\left(\mu_e\left(\frac{\partial v}{\partial x}\right)\right)$
y-momentum	v	μ_e	$-\frac{\partial p}{\partial y}+\frac{\partial}{\partial y}\left(\mu_e\left(\frac{\partial v}{\partial y}-\frac{2}{3}\left(\frac{\partial u}{\partial x}+\frac{\partial v}{\partial y}\right)\right)\right)+\frac{\partial}{\partial y}\left(\mu_e\left(\frac{\partial u}{\partial y}\right)\right)-g(\rho-\rho_0)$
Kinetic energy	κ	Γ_κ	Gs - $\rho\varepsilon$
Dissipation rate	ε	Γ_ε	$\frac{\varepsilon}{\kappa}(C_1 Gs)+C_2\rho\frac{\varepsilon^2}{\kappa}$
Energy	**T**	Γ_e	$\frac{Gs}{c_p}$
Equation of state	$p = p(\rho, T)$ and $p = \rho RT$		

The effective viscosity coefficient, μ_e, is defined by:

$$\mu_e = \mu + \mu_\tau$$

The production term Gs is defined by:

$$Gs = \mu_\tau \left[2 \left[\left(\frac{\partial u}{\partial x}\right)^2 + \left(\frac{\partial v}{\partial y}\right)^2 \right] + \left(\frac{\partial u}{\partial x} + \frac{\partial v}{\partial x}\right)^2 \right] - \frac{2}{3}\left(\left(\frac{\partial u}{\partial x} + \frac{\partial v}{\partial y}\right) \right)^2$$

and the energy diffusion coefficient is

$$\Gamma_e = \frac{k}{c_p}$$

3-2 Turbulence Models

The majority of the classical turbulence models used in solving turbulent flow problems are based on μ_τ and the turbulent diffusivity concepts. Three different turbulence models, namely Standard k-ε, RNG k-ε, and Realizable k-ε are used to select the suitable turbulence model. The computational results from different turbulence models are compared with several published experimental data to select the suitable turbulence model with the present study.

4- Grid Generation.

The simulation of flow domain through the blade passage is important to predict the flow properties. The domain is created based on the different geometries of the blades. An inventor 2-D is used to create the blade profiles and the structured mesh for the computational domain. The commercial grid generator ICEM (application of CFD) is used. During the meshing process, the multi-block technique is utilized. The grid generation is all Quad type with 60,000-grid points, the flow path between two blades is created as shown as in Fig (3). From the figure it can be noticed that the grid is condensed near the suction and pressure surfaces of the blade to give a good predication of the flow aerodynamic properties near blade surface. Extended domain is taken in consideration before inlet (leading edge) and after blade (trailing edge) to simulate the flow properties in the complete domain as shown as Fig (3).

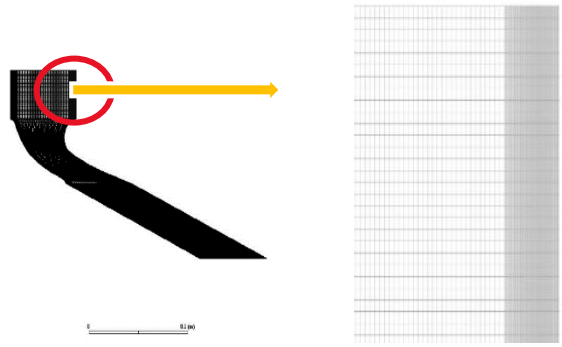

Fig. (3) Computational grid of blade cascade

5-Boundary Condition

To solve the governing equations, the boundary conditions as shown in Fig (4) are used. The inlet boundary condition is pressure inlet and normal on the inlet surface. Both sides of the inlet domain are created and defined as periodic boundary condition. Both suction and pressure sides are stationary and adiabatic walls. The exit section is extended tangentially with camber line to describe the flow properties after exit. The outlet conditions are assumed the pressure outlet and equal to atmospheric pressure. Also the two sides of extension exit domain are periodic boundary conditions.

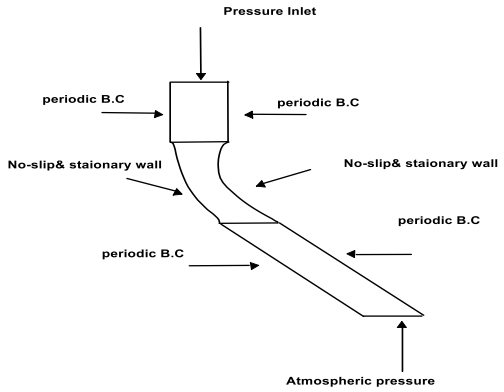

Fig. (4) Computational domain and boundary conditions.

For investigating the behavior of the turbulence models near a solid boundary, analysis to determine limiting forms of the equations near the wall is considered, y^+. It's values are between $5 < y^+ < 30$ for all the tested geometries.

6- Theoretical Model Validation

The literature review indicated that, there is no one turbulence model used to describe the flow properties through turbine cascade. Some studies concluded that standard k-ε model is valid and others research recommended with RNG k-ε model. In the other hand some studies presented realizable k-ε is more suitable to predict the flow patterns inside turbine cascade. Therefore, the three turbulence models are used to simulate the flow properties through the turbine blade passage and select the more suitable turbulence model during present study. A comparison between the theoretical results of the three turbulence models with experimental published data [17] is presented in Fig (5). This figure indicates change of pressure coefficient on both surfaces of turbine blade along axial chord.

The pressure coefficient can be calculated using following equation:

$$C_p = \frac{p - p_{ref}}{p_0 - p_{ref}} \quad \ldots\ldots\ldots\ldots\ldots \quad (2)$$

Where p is the local static pressure p_0 is the total pressure and p_{ref} is the reference pressure.

The criteria of convergence in this study are that the residual is 10^{-5} for the continuity and momentum equation and 10^{-6} for the energy equation. From the figure, it can be noticed that, all tested turbulence models have the ability to predict the flow behavior with different degree of accuracy.

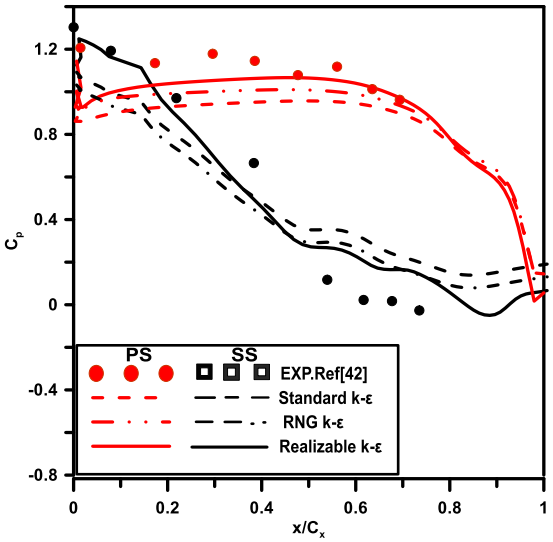

Fig.(5) Comparison between numerical results using different turbulence models with experimental published data [17].

To judge the more suitable turbulence model, the correlation coefficient (R^2) is used. The correlation coefficient is defined as:

$$R^2 = 1 - \frac{Difference\ between\ measured\ and\ predicted\ parameter}{Experimental\ results\ deviation}$$

$$= 1 - \frac{\sum(\varphi_{measured} - \varphi_{predicted})^2}{\sum(\varphi_{Exp} - \underline{\varphi_{Exp}})^2} \quad \ldots\ldots\ldots \quad (3)$$

where, $\varphi_{measured}$ is the measured value of flow parameter at a certain point in the domain and $\varphi_{predicted}$ is the predicted value of the same flow parameter at the same point. $\underline{\varphi_{Exp}}$ is the mean value of parameter, which can be defined as follow:

$$\underline{\varphi_{Exp}} = \frac{\sum_{i=1}^{n} \varphi_{Exp}}{n}$$

where, n is the number of experimental points.

Based on the theoretical and experimental results, (R^2) is calculated for each turbulence model and presented in table (3). The high values of correlation coefficient indicate high accurate numerical results.

Table (3) The correlation coefficient R^2 of turbulence models.

Turbulence model	Correlation coefficient R^2
Standard k-ε	**0.981704**
RNG k-ε	**0.967639**
Realizable k-ε	**0.994732**

From table (3) it can be noticed that the realizable k-ε gives the higher value of R^2, so the realizable k-ε model will be used to extend all computations in the present study.

For more validation of CFD model, with using (Realizable k-ε) turbulence model, another comparison is performed with three different published data. The first comparison is performed with Sun et al. [17] data. The geometry of blade in ref. [17] is created and used with the same dimension (i.e. chord length = 38.67 mm, axial chord=30 mm, pitch =27.92 mm) and same operating conditions (i.e. incidence angle = -41°, -16° degree, and exit Mach number = 0.75). A comparison between the present predicted results and the measured -pressure coefficient distributions along the pressure and suction blade surfaces at incidence angle= -41° and -16 ° are shown in Fig.(6-a) and Fig (6-b), respectively. From the figure it can be noticed that acceptable agreement between the current numerical results and both of experimental and theoretical data with Ref [17].

The second validation of the present numerical model with theoretical and experimental results of Pacciani et al. [4] is investigated. The dimension of Pacciani's geometry is pitch/chord ratio =1.05, inlet flow angle =34.7 °. The boundary conditions are pressure inlet = 0.8 bar, pressure outlet= 0 bar, turbulence intensity =4%, Mach number=0.7. The values of pressure coefficient on pressure and suction surface of the blade using present turbulence model and published theoretical and experimental data are shown in Fig (7). From this figure it can be declared that there is fair agreement between present model and published results.

Another validation of the theoretical model is performed by comparing the distribution of Mach number at axial plane downstream of the trailing edge with theoretical and experimental results of Sanz et al [8]. Geometry and boundary conditions of reference [8] are created and applied with dimensions, the chord length = 58 mm, axial chord length = 48.4 mm, pitch = 41.8 mm and turbulence intensity=2.5%. From fig. [8] it can be seen that the present model provides considerable agreement between the present

theoretical results compared with the published experimental results.

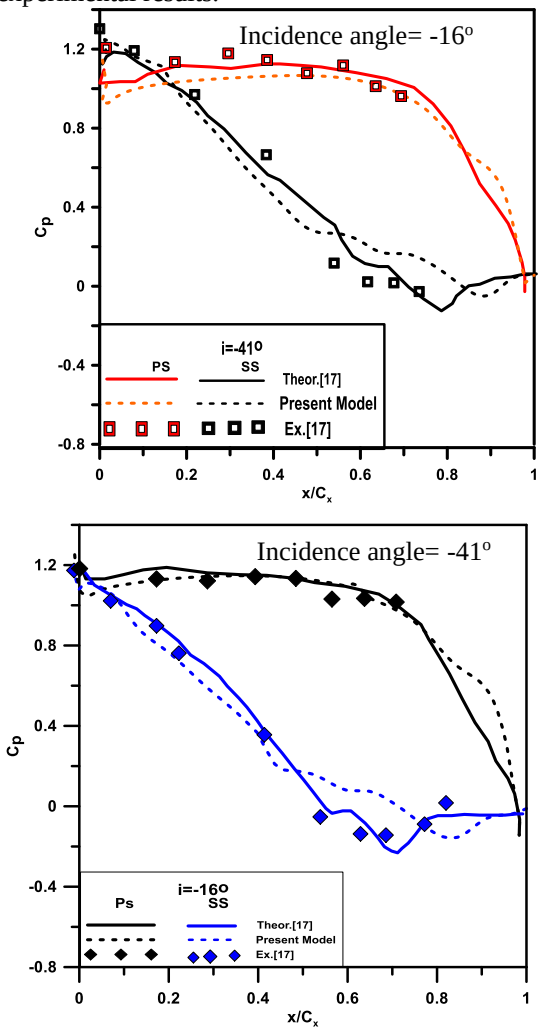

Fig. (6) Comparison between present numerical and previous published results [17].

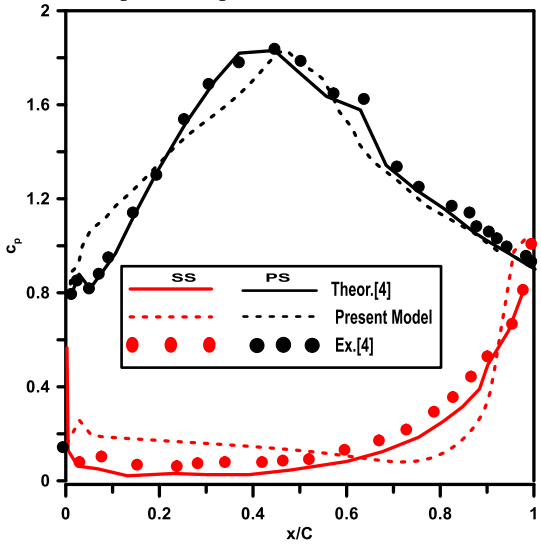

Fig. (7) Comparison between present numerical results and previous present Results [4].

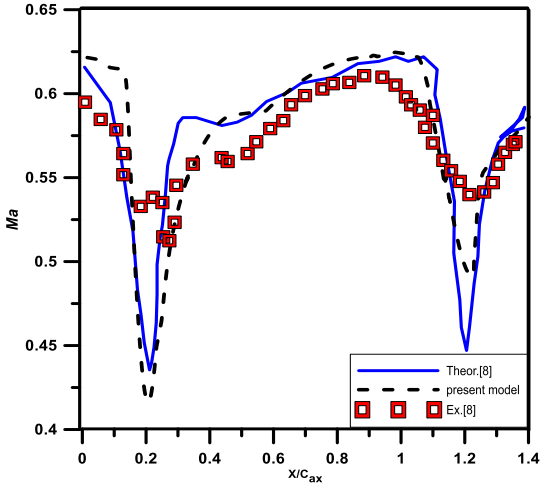

Fig. (8) Comparison between present numerical results and previous published data [8]

From the previous comparisons, it can be concluded that the suggested CFD model (ANSYS 17 software) with using Realizable k-ε model can be used to simulate and predict the flow properties through the passage of turbine blades.

7- Computational Results

The effect of some geometric parameters and operating conditions such as the position of maximum camber position of turbine blade and inlet Reynolds number on the flow properties and aerodynamic performance will be studied. The flow properties include Mach number distribution, pressure coefficient distribution on pressure and suction surfaces of the blade, pressure loss coefficient and blade-loading coefficient.

7-1 Effect of maximum camber position

The effect of changing the maximum comber position on the pressure coefficient distribution along the pressure and suction surfaces of the turbine blade and the Mach number distribution through the blade passage for different blade geometry will be presented in following section.

7.1.1 Pressure coefficient distribution.

The effect of changing maximum camber position on C_p distribution along the pressure and suction surfaces of the blade at constant value of Rei=7.6×105 (⟦Re_i=7.6×10^5 ($Re_i = \frac{\rho_i U_i C}{\mu}$ where ρ_i is inlet density and U_i is inlet velocity) , S/C=0.9 and i=0° is shown in Fig. (9). From the figure it can be noticed that the C_p distribution on pressure surface is almost the same for all geometries from leading edge of the blade to x/C_x≅0.68 then decreases rapidly to

reach the trailing edge. Also, it can be observed that, changing the position of maximum camber of the turbine blade has greatly effect on the distribution of the pressure coefficient on the suction surface of the turbine blade in the region from leading edge of the blade until reaching the position of lowest value of the pressure coefficient, then this effect decreases in the region between the lowest value for the pressure coefficient and blade exit. This performance can be explained as a result of a change in the shape of the suction surface of the turbine blade and consequently the area available for flow through the blade passage.

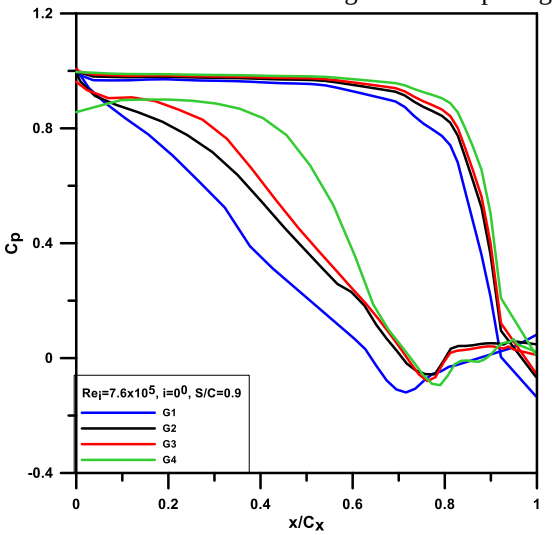

Fig (9) Pressure coefficient distribution C_p along axial chord for all tested blade geometries at Rei= 7.6×10^5, i=0° and S/C=0.9.

7.1.2 Mach number contours

The Mach number contours inside the blade passage is shown in Fig. (10). From the figure it can be noticed that, the Mach number has low value at the inlet and it increases with progressing through blade passage. Mach number value reaches to unity (i.e. Ma =1.0) at the minimum area of all blades and it continuous to increase in downstream direction until exit from blade passage. Also, the figure shows the effect of blade geometry on the Mach number contours through the blade passage.

From this figure it can be noticed that, the Mach number at exit section of the blade for G1 is low compared with other geometries G2, G3 and G4 as a result of changing maximum camber position. Also, it can be observed that for geometry G2, G3 and G4, separation zone is appeared at the last part of the suction blade. The separation zone is increased with changing the maximum camber position (G2, G3 and G4 respectively). Also from this figure it can be noticed that, changing the maximum camber position of the blade (G4) towards to the trailing edge attributed to the accelerated separation of the boundary layer on the suction surface of the blade and consequently increased the size of separation region near the trailing edge.

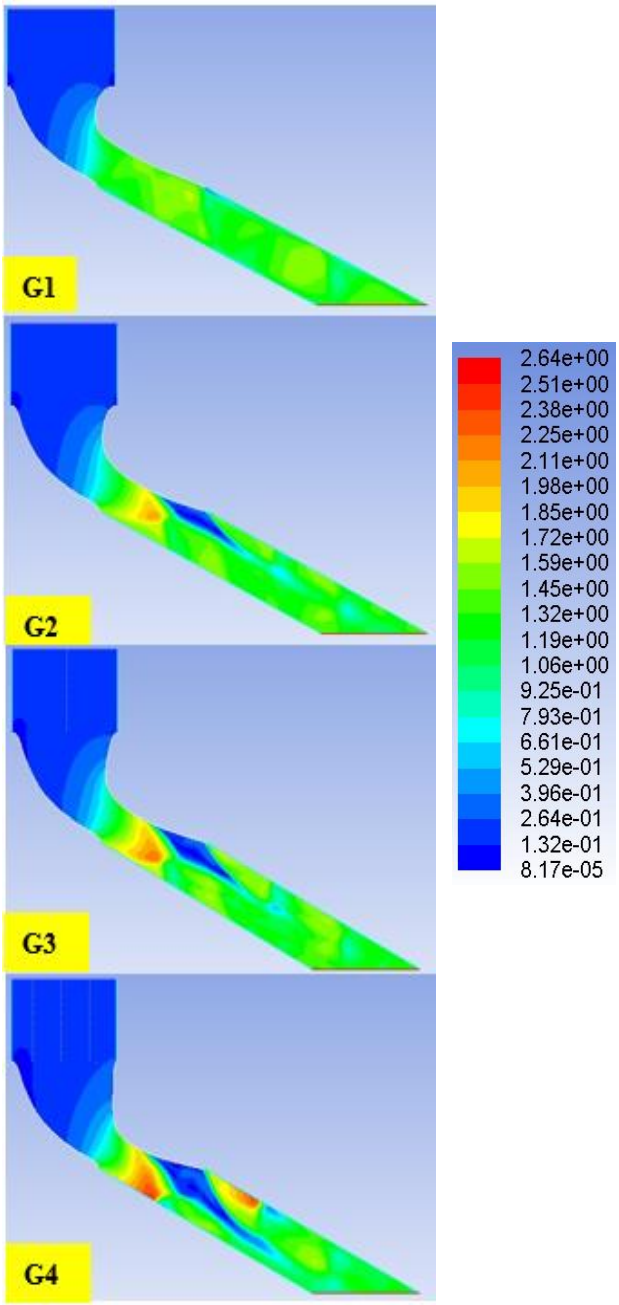

Fig (10) Distribution of Mach number contours for all different tested geometries at Rei=7.6×10^5, i=0° and S/C=0.9.

7-2 Lift and Drag Coefficients

Based on numerical results for flow characteristics through the blade passage and the weighted average values of velocity and density at exit of blade passage,

the drag and lift coefficient are calculated as following:

$$C_d = \frac{F_D}{0.5*\rho*v_2^2*A} \quad \ldots\ldots\ldots \quad (4)$$

$$C_L = \frac{F_L}{0.5*\rho*v_2^2*A} \quad \ldots\ldots\ldots \quad (5)$$

Where F_D, F_L are the drag and lift forces and *v2* is the outlet velocity of flow from the blade passage.

The change of lift and drag coefficients at zero incidence angle and pitch chord ratio 0.9 with inlet Reynolds number for all tested geometries are shown in Fig (11). From this figure it can be noticed that the lift coefficient increases with increasing inlet Reynolds number for all blade geometries, the drag coefficient increases with increasing inlet Reynolds number in the range of 3.77 to 12.8x10^5 for all blade geometries. Also, this figure shows the high value of C_L and C_d for G1, this behavior reflects the effect of changing position of maximum camber position.

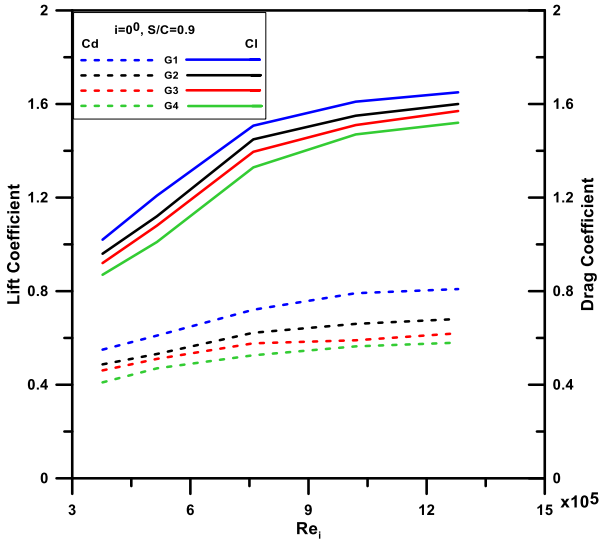

Fig (11) Variation of lift and drag coefficients with Re for different blade geometry

7-3 Pressure loss coefficient

The pressure loss coefficient (Y_p) is defined as the ratio between the total pressure difference ($P_{o1} - P_{o2}$) across the blade passage and the outlet dynamic pressure of the flow.

$$Yp = \frac{\Delta p_0}{0.5*\rho*v_2^2} \quad \ldots\ldots\ldots \quad (6)$$

Where *v2* is the velocity at outlet of the blade.

Based on numerical results of the flow characteristics through blade passage, the weighted average values of both total pressure at inlet and outlet of blade passage are calculated and used to determine Y_p. Fig (12) shows changing of Y_p with inlet Reynolds number for different blade geometries. From this figure it can be noticed that, the pressure loss coefficient decreases with increasing inlet Reynolds number. Also, Fig (12) declared that, the blade geometry G1 has the minimum value of Y_p compared with other blade geometries.

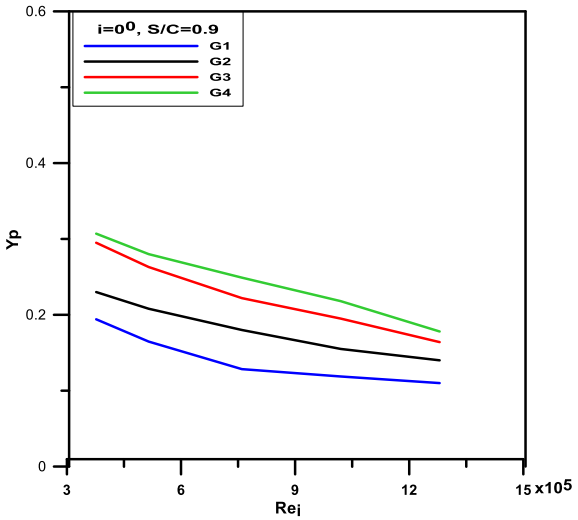

Fig (12) Change of pressure loss coefficients for different blade geometries with Re.

7-4 Loading Coefficient

The blade loading coefficient (L_c) is the most important design parameter in turbomachinery blades. It is defined as following:

$$L_c = \frac{\int_0^1 (p_p - p_s) d\left(\frac{x}{C_x}\right)}{(p_{01} - p_{o2})} \quad \ldots\ldots \quad (7)$$

Where p_{01} is the total pressure at inlet of the blade cascade and p_{o2} is the outlet total pressure.

Figure (13) shows the relation between the loading coefficient and the changing of inlet Reynolds number from 3.77 to 12.8x10^5. From this figure it can be illustrated that, the blade loading coefficient decreases with increasing the values of inlet Reynolds number due to change of flow characteristics through the blade passage. Also, fig. (13) declared that the blade geometry G1 has the maximum value of loading coefficient compared with other blade geometries.

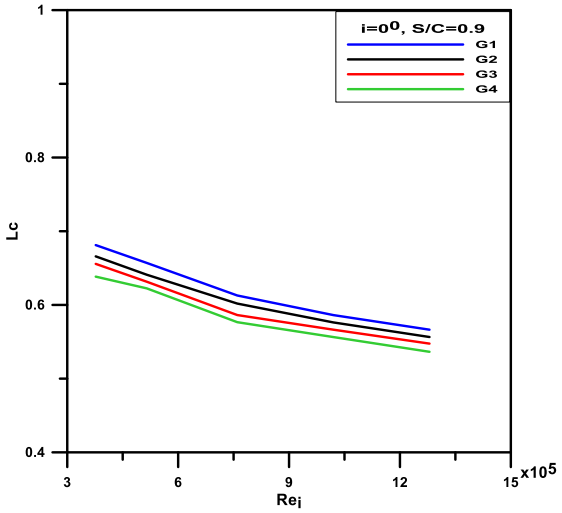

Fig (13) Change of blade loading coefficient with different values of Re for all tested blades.

8- Conclusions

From the previous discussion, it can be concluded that,

- Among the most turbulence models used in predicting flow through blades passage (Standard k-ε, RNG k-ε, and Realizable k-ε), Realizable k-ε model is more suitable to predict and simulate the flow parameters through the blade passage.
- Changing the maximum camber position of the turbine blade significantly affects the pressure coefficient on the suction surface of the blade while its effect is small on the pressure surface of the turbine blade at different operating conditions.
- The separation zone on the suction surface of the blade occurs near the trailing edge and its size increases with changing the maximum camber position of the blade towards the trailing edge.
- The lift and drag coefficients increase with increasing inlet Reynolds number, Rei, and their values are depended on the position of maximum camber.
- The pressure loss coefficients for different tested blade geometries decreases with increasing inlet Reynolds number Rei, and its minimum value occurs when the maximum camber position is close to the leading edge of the blade, G1.
- Finally, the best aerodynamic performance for tested blades geometry at pitch/chord ratio 0.9, and incidence angle i=0o occurs at maximum camber position about 0.157 away from leading edge.

NOMENCLATURE

C	Chord	(mm)
C_x	Axial cord	(mm)
C_p	Pressure coefficient	(-)
C_d	Drag coefficient	(-)
C_L	Lift coefficient	(-)
F_D	Drag force	(N)
$\mathbf{F_L}$	Lift Force	(N)
i	Incidence angle	deg
I	Turbulence intensity	
K	Turbulent kinetic energy	(m^3/s^2)
L	Length of chord line	(mm)
$\boldsymbol{L_c}$	Blade loading coefficient	(-)
Re_i	Inlet Reynolds number	(-)
s	Pitch (Blade Spacing)	(mm)
t_m	Maximum thickness of the blade	(mm)
u	Velocity component in x-direction	(m/s)
v	Velocity component in y-direction	(m/s)
x	Length of surface	
Y_p	Pressure losses coefficient	(-)

Greek symbols

Γ	Diffusion coefficient	(m^2/s)
Φ	Scalar quantity	
ε	Turbulent dissipation rate	(m^2/s^3)
μ	Dynamic viscosity	(kg/m .s)
μ_τ	Turbulent diffusivity	
ρ	Density	(kg/ m^3)

Abbreviations

CFD	Computational fluid dynamics
Ma	Mach number
p_s	pressure surface
Re	Reynolds number
RNG	Re-normalization group
ss	suction surface

9- References

[1] V.G.Gribin, A.A.Tishchenko, L.Y.Gsvrilov, R.A.Alexeev" Turbine blade profile design using Bezier curves" Turbomachinery fluid dynamics, Sweden, 2017.

[2] S.V.R.Murthy, S.K.Kumar" Development and validation of a Bezier curve based profile generation method for axial flow turbines "International Journal of scientific , 2014, pp. 187-192.

[3]J. Dunham" A parametric method of turbine blade profile design, the profile shape of an axial turbine" ASME (American Society of mechanical engineering), 1974, pp. 1-8.

[4] P.Pacciani, M.Marconcini, A.Arnone, F.Bertini" An assessment of the laminar kinetic energy concept for the prediction of high-lift, low-Reynolds number cascade flows "journal of power and energy,2011, Vol. 225 Part A, pp. 995-1003.

[5] G.Medic, O.Sharma" Larg eddy simulation of flow in a low pressure turbine cascade" ASME Turbo Expo 2012, Denmark, pp 1-10.

[6] V.Michelassi, J.Wissink, W.Rodi"Analysis of DNS and LES of Flow in a Low Pressure Turbine Cascade with Incoming Wakes and Comparison with Experiments" Kluwer academic publishers, 2003, pp. 295-330

[7] D,B.M.Jouini, S.A.Sjolander, S.H.Moustapha" Aerodynamic Performance of a Transonic Turbine Cascade at Off-Design Conditions " journal of turbomachinery,2001, pp. 510-517.

[8] W.Sanz, H.Gehrer, J.Woisetschagern, M.Forstner, W.Artner, H.Jericha" Numerical and Experimental investigation of the wake flow downstream of a linear turbine cascade" ASME International Gas Turbine and Aeroengine Congress, Stockholm, Sweden, pp.1-10.

[9] V.Dossena, G.DL,ppolito, E.Pesatori" Stagger angel and pitch chord ratio effect on secondary flow downstream of a turbine cascade at several off-design conditions" ASME TURBO EXPO 2004, Austria, 2004, pp.1-10

[10] B.Ghazanfari, M.N.Ahmadabadi, A.T.Farasani, M.H.Noorsalehi" Numerical study of camber and stagger angle effects on the aerodynamic performance of tandem-blade cascades" Elsevier journal, 2017, pp. 30-42.

[11] Z.Zhou, S.Chen, W.Li, S.Wang, X.Zhou" Experiment study of aerodynamic performance for the suction-side and pressure-side winglet-cavity tips in a turbine blade cascade" Elsevier journal, 2018, pp. 220-230.

[12] C.Bode, T.Aufderheide, D.Kozulovic, J.Friedrichs" The effect of turbulence length scale on turbulence and transition in turbomachinery flows" ASME TURBO EXPO 2014, Germany, June2014, pp.1-13

[13] A.F.Nemnem, M.G.Turner" Smooth curvature of airfoils mean lone for a general turbomachinery geometry generator" Aerospace Sciences & Aviation Technology, 2015, pp. 116-142.

[14] T.Korakiantis, P.Papagiannidis" Surface curvature distribution effects on turbine cascade performance" ASME, 1992, pp. 84-92.

[15] Y.C.Nho, J.S.Park, Y.J.Lee, J.S.Kwak" Effect of turbine blade tip shape on total pressure losses and secondary flow of a linear turbine cascade" international journal of heat fluid flow, 2012, pp. 92-100.

[16] H.Sun, J.Li, Z.Feng" Investigations on Aerodynamic Performance of Turbine Cascade at Different Flow Conditions "Taylor and Francis group, 2014, pp. 214-223.

[17] H.D.Akolekar, F.Waschkowski, Y.Zhao, R.Pacciani, R.D.Sandberg" The transition modeling for low pressure turbines using computational fluid dynamics driven machine learning" Multidisciplinary Digital Publishing Institute Journal, 2021, pp.1-16

[18] Y.Yining" Analysis of the influence of camber on hydrodynamic characteristic of airfoil" Journal of Physics, 2020, pp.1-9.

[19] R.Rgjnish, N.S.Thakur, P.K.Pant "Effect of camber and angles of attack on airfoil charactristics." Journal of Engineering and technology, 2024, pp. 729-736

[20] Y.Kim, M.Park, J.Lee, H. Choi, S. Kang "Effect of Incidence Angle on Gas Turbine Blade Performance." Aerospace Science and Technology, 2021, pp.

[21] H.K.Versteeg, W.Malalasekera" An Introduction to computational fluid dynamics" Second editor, Pearson education limited, 2007.

[22] S.M.Yahya" Turbines, compressors and fans" Newdelhi, 2011.